Preparation, characterization of ZrO$_x$N$_y$/C and its application in PEMFC as an electrocatalyst for oxygen reduction

Gang Liu [a,b], Hua Min Zhang [a,*], Mei Ri Wang [a], He Xiang Zhong [a,b], Jian Chen [a]

[a] *Lab of PEMFC Key Materials and Technologies, Dalian Institute of Chemical Physics, Chinese Academy of Sciences, Dalian 116023, China*
[b] *Graduate School of the Chinese Academy of Sciences, Beijing 100039, China*

Abstract

In this paper, a noble-metal-free electrocatalyst based on carbon-supported zirconium oxynitride (ZrO$_x$N$_y$/C) was prepared by ammonolysis of carbon-supported zirconia (ZrO$_2$/C) at 950 °C and investigated as cathode electrocatalyst towards oxygen reduction reaction (ORR) in PEMFCs. The electrocatalyst was characterized by X-ray diffraction (XRD) and transmission electron microscopy (TEM) techniques. The catalytic activity of the catalyst towards ORR was investigated by using the rotating disk electrode (RDE) technique in an O$_2$-saturated 0.5 M H$_2$SO$_4$ solution. The ZrO$_x$N$_y$/C electrocatalyst presented attractive catalytic activity for ORR. The onset potential of ZrO$_x$N$_y$/C electrocatalyst for oxygen reduction was 0.7 V versus RHE and the four-electron pathway for the ORR was achieved on the surface of ZrO$_x$N$_y$/C electrocatalyst. The ZrO$_x$N$_y$/C electrocatalyst showed a comparatively good cell performance to ORR in PEMFCs, especially when operated at a comparatively high temperature. © 2007 Elsevier B.V. All rights reserved.

Keywords: Zirconium oxynitride; Noble-metal free electrocatalyst; Oxygen reduction reaction; Cathode; Fuel cell

1. Introduction

Proton exchange membrane fuel cells (PEMFCs) are regarded as a possible alternative power source for stationary and mobile applications, due to their high-power density and near-zero pollutant emission [1]. However, there are several problems including the large overpotential of the ORR and the high cost of the electrocatalysts to be solved before commercialization can occur [2]. The reaction occurring at the cathode of the PEMFC is the reduction of oxygen in the presence of protons and electrons to produce water [Eq. (1)]:

$$O_2 + 4H^+ + 4e^- \rightarrow 2H_2O \qquad (1)$$

Currently, the common used cathode electrocatalysts for PEMFC are carbon-supported platinum. In order to improve the ORR activity of platinum electrocatalysts, platinum transition metal alloys have been well developed [3–5]. However, the stability of alloy electrocatalysts becomes a serious problem for long-term operation for transition metals tend to dissolve in acid electrolyte [6,7]. Moreover, the price of Pt is very high. So a strong motivation exists to find less expensive non-noble metal alternatives that are stable and exhibit catalytic activity comparable to that of Pt. Various materials have been proposed as non-noble cathode electrocatalysts for ORR. Such as, transition metal oxides [8], transition metal (e.g., Fe, Co) macrocyclic compounds [9], Ru-based chalcogenides [10] and etc. Unfortunately, neither of these electrocatalysts has reached the catalytic activity of Pt-based electrocatalysts and virtually none has sufficient stability in the acidic environment of PEMFC.

Transition metal nitrides as corrosion resistance materials have attracted much attentions over the years [11,12]. Transition metal nitrides have been studied as ORR electrocatalysts because of their high stability in acid medium and platinum-like catalytic behavior [13,14]. Herein we reported the results of a study on the electrocatalytic activity of zirconium oxynitride for ORR. The ZrO$_x$N$_y$/C electrocatalyst was prepared by ammonolysis of ZrO$_2$/C at 950 °C. The ORR activities of this electrocatalyst were evaluated by RDE measurements and single cell tests. The stability of the electrocatalyst was also investigated in the single cell test. The ZrO$_x$N$_y$/C electrocatalyst showed promising ORR activity and stability, and might have the possibility to be an alternative of the Pt-based electrocatalysts.

* Corresponding author. Tel.: +86 411 8437 9072; fax: +86 411 8466 5057.
E-mail address: zhanghm@dicp.ac.cn (H.M. Zhang).

2. Experiment

2.1. Preparation of carbon-supported zirconium oxynitride electrocatalyst

The carbon-supported zirconium oxynitride electrocatalyst was prepared by ammonolysis of carbon-supported zirconia at 950 °C as presented by Gilles and Collongues [15]. The preparation process of the electrocatalyst was composed of two steps: the preparation of ZrO_2/C and the ammonolysis of ZrO_2/C. The detailed process was as follows. One gram Vulcan XC-72 carbon powder (Cabot Corp., BET: $235\,m^2\,g^{-1}$, denoted as C) was added to the 155 mL aqueous solution containing 5 mL ethanol and 150 mL water. The solution was mixed sufficiently before $0.5422\,g\,ZrO(NO_3)_2\cdot2H_2O$ was added. The mixture was treated in an ultrasonic bath to form uniformly dispersed ink. The ink was then dried at 90 °C. The dried mixture was heat-treated at 500 °C in N_2 for 3 h to get ZrO_2/C (20 wt.% ZrO_2). The carbon-supported zirconium oxynitride (ZrO_xN_y/C) was synthesized by heating ZrO_2/C at 950 °C in NH_3 for 3 h. When the reaction was over, the sample was cooled to room temperature under N_2 atmosphere and the electrocatalyst ZrO_xN_y/C (about 20 wt.% ZrO_xN_y) was thus obtained.

2.2. Physicochemical characterization

XRD measurements were conducted on a PAN-alytical powder diffratometer (Philips X'Pert PRO) using Ni filtered Cu Kα radiation ($\lambda = 1.54056\,Å$) to characterize the structures of XC-72 Carbon, ZrO_2/C and ZrO_xN_y/C electrocatalyst.

TEM image was recorded on a JEOL JEM-2000EX microscope operated at 120 kV. The electrocatalyst powder was placed in a vial containing ethanol and then ultrasonically agitated to form homogeneous slurry. A drop of the slurry was dispersed on a holey polyvinyl formal microgrid for the TEM analysis. Two hundred particles were calculated to obtain the integrated information about the overall distribution of the electrocatalyst.

2.3. Electrochemical characterization

Eeletrochemical measurements were carried out on CHI 660 electrochemical station (CH Corporation, USA) with a RDE system (EG&G model 636). A standard three-electrode cell was used. A Pt foil was served as counter electrode and a saturated calomel electrode (SCE) was used as reference electrode. The electrocatalyst layer on the glassy carbon electrode (GCE) (4 mm in diameter) was prepared as follows: a mixture containing 1 mL of ethanol, 5 mg of XC-72 carbon or ZrO_2/C or ZrO_xN_y/C or Pt/C (20 wt.%, Johnson Matthey) and 50 μL of Nafion solution (5 wt.%) was homogenized for 30 min in a ultrasonic bath. 25 μL of the mixture was cast on the clean GCE surface and dried in air. The electrochemical measurements were carried out in 0.5 M H_2SO_4 solution at room temperature. All potentials shown in the figures were quoted to RHE. The cyclic voltammetry (CV) curves were recorded in the potential range from 0.05 to 1.2 V versus RHE with a scan rate of $100\,mV\,s^{-1}$

after bubbling high-purity nitrogen through the electrolyte for 30 min. The RDE curves were obtained in the scan range from 1.0 to 0.05 V versus RHE with a scan rate of $5\,mV\,s^{-1}$ after O_2 bubbling for 30 min.

To validate whether Pt from the counter electrode will contaminate the working electrode and invalidate the results, we carried out the CV and RDE measurements on ZrO_xN_y/C electrocatalyst in the three-electrode system by the use of graphite rod as the counter electrode.

2.4. Preparation of membrane electrode assembly and single cell test

The electrode was prepared as follows: mixing ZrO_xN_y/C electrocatalyst, 5% Nafion and ethanol to form a homogeneous mixture, spraying the mixture onto the wet-proofed carbon paper (SGL, 39% PTFE). The ZrO_xN_y loading in the electrode was about $1\,mg\,cm^{-2}$ and the dry Nafion loading was about $0.5\,mg\,cm^{-2}$. This electrode was used for the cathode. The ZrO_2/C or Pt/C cathode was prepared by the same procedure. The ZrO_2 loading in the ZrO_2/C cathode was about $1\,mg\,cm^{-2}$ and the dry Nafion loading was about $0.5\,mg\,cm^{-2}$. The Pt loading in the Pt/C cathode was about $0.4\,mg\,cm^{-2}$ and the dry Nafion loading was about $0.2\,mg\,cm^{-2}$. The anode adopted the commercial 46.7% Pt/C electrocatalyst (TKK Co.) with Pt loading of $0.37\,mg\,cm^{-2}$ and Nafion 117 (175 μm, Du Pont) was used as the membrane. The MEA was fabricated by hot-pressing the anode and the cathode to the membrane at 140 °C and 1 MPa for 1 min and fitted into a test station. The active area of the MEA was $5\,cm^2$. The single cell performance was tested at 80, 60 and 40 °C with saturated humidification level. The single cell was fed with pure hydrogen and oxygen and operated at 0.2 MPa. Fifty-hour stability tests of single cells with ZrO_xN_y/C and Pt/C as cathode electrocatalysts were also carried out at 80 °C with a constant current density of $200\,mA\,cm^{-2}$.

3. Results and discussion

3.1. XRD and TEM characterization of carbon-supported zirconium oxynitride

Fig. 1 shows the XRD patterns of XC-72 carbon, ZrO_2/C and ZrO_xN_y/C electrocatalyst. As shown in Fig. 1, the first peak at the low 2θ range ($2\theta = 25°$) was associated with the XC-72 carbon support. ZrO_2/C showed the typical tetragonal zirconia crystal structure with some monoclinic phase impurities [16]. The structure of ZrO_xN_y/C was β''-phase zirconium oxynitrides with non-regular succession of the basic building units of β-phase $Zr_7O_8N_4$ and monoclinic phase ZrO_2 [17].

Fig. 2a shows the typical TEM image of the ZrO_xN_y/C electrocatalyst and the histogram of the particle size distribution was shown in Fig. 2b. The amorphous carbon appeared as the gray areas and the ZrO_xN_y particles appeared as the black particles. Due to the high temperature heat treatment, the ZrO_xN_y particles size distribution is very broad and ranges between 6 and 14.5 nm. The mean particle size is about 9 nm.
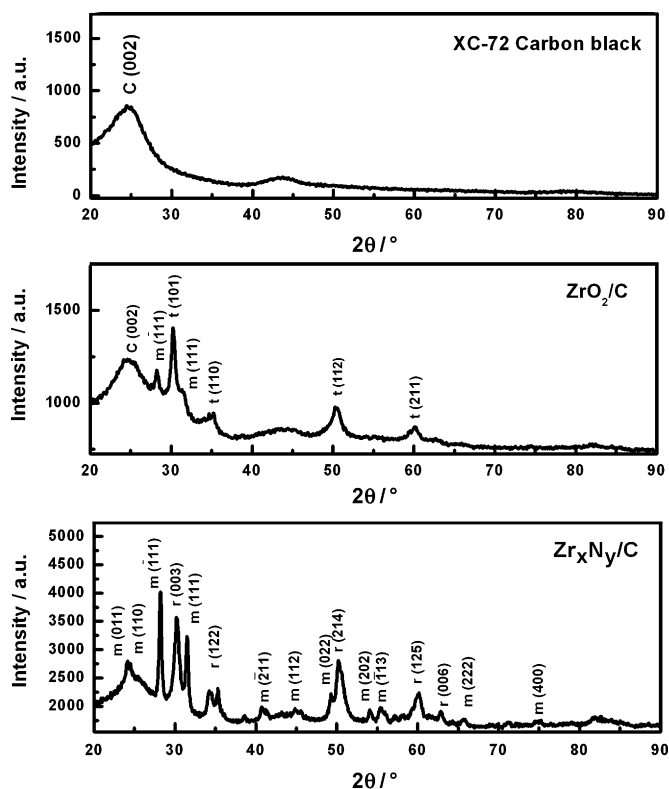
Fig. 1. XRD patterns of XC-72 Carbon, ZrO_2/C and ZrO_xN_y/C electrocatalyst. m: m-ZrO_2, t: t-ZrO_2, r: β-phase $Zr_7O_8N_4$.

3.2. Electrochemical measurements of the electrocatalysts

The CVs from the first to the tenth cycle of the ZrO_xN_y/C catalyst under nitrogen atmosphere was shown in Fig. 3. The ZrO_2/C sample showed almost the same CV behavior. The oxidation and reduction peaks at about 0.6 V was responsible for the carbon support. No other specific oxidation and reduction current peaks were observed. The CVs soon approached to a steady state. The anodic and cathodic charges of the CV were 24.0 and 24.5 mC cm^{-2}, respectively. These results indicate that ZrO_xN_y is stable in acid solution at least in the potential range from 0.05 to 1.2 V.

In order to investigate the electrocatalytic activities of the electrocatalysts for ORR, RDE measurements were carried out both in N_2 and O_2 atmosphere, respectively. Fig. 4 shows the linear scan voltammogram (LSV) curves of electrodes (a) bare GCE, (b) XC-72 R/GCE, (c) ZrO_2/C/GCE and (d) ZrO_xN_y/C/GCE in 0.5 M H_2SO_4 electrolyte saturated with N_2 and O_2 at room temperature. As shown in Fig. 4, very low currents were observed in the potential range for all the electrodes under the N_2 atmosphere. Comparatively, the reduction currents increased for all the electrodes under the O_2 atmosphere. The potential at which the reduction current with bare GCE under O_2 increased more than that under N_2 was about 0.55 V. Unfortunately, the reduction current was very low owing to the scarce active sites for ORR on bare GCE. The ORR onset potentials for the XC-72 carbon and ZrO_2/C were about 0.55 and 0.56 V, respectively. The reduction current on the ZrO_2/C/GCE electrode was a little higher than that on the XC-72 R/GC electrode.
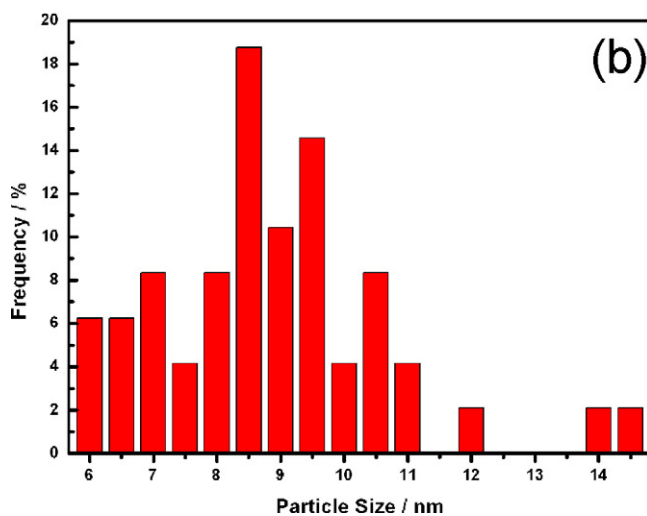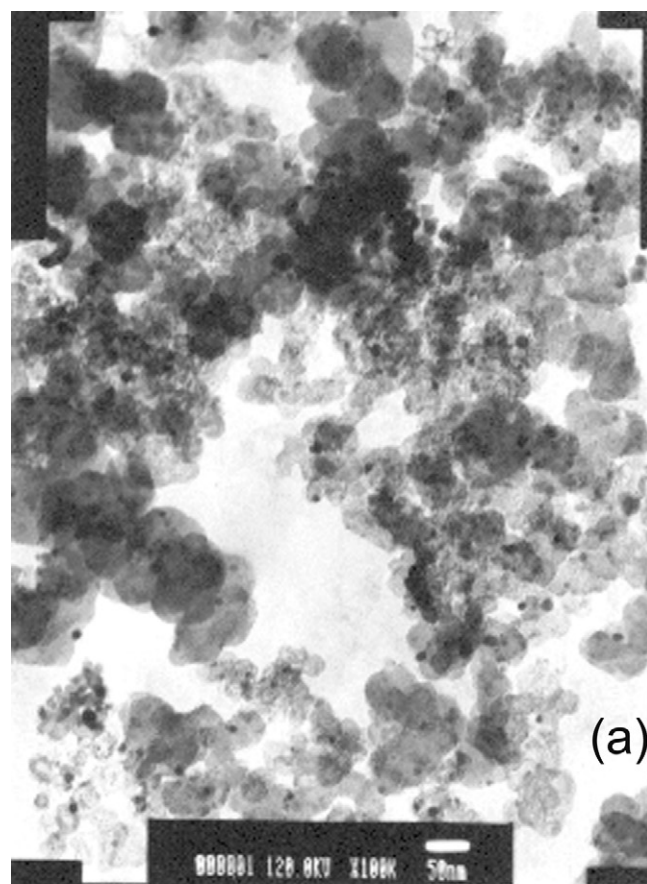

Fig. 2. TEM image (a) and histogram (b) of the particle size distribution of the ZrO_xN_y/C electrocatalyst.

The above two electrodes showed higher reduction current than bare GCE, but the reduction current was still very low. However, as shown in Fig. 4d, the reduction current with ZrO_xN_y/C under O_2 started at about 0.7 V. Because such a reduction current was not observed under N_2 atmosphere, the reduction current should be due to the oxygen reduction. ZrO_xN_y/C had attractive ORR activity and the reduction current was the highest among the four tested electrodes. Liu et al. [18] and Doi et al. [19] investigated the ORR activities of sputtered ZrO_2 and ZrO_xN_y.
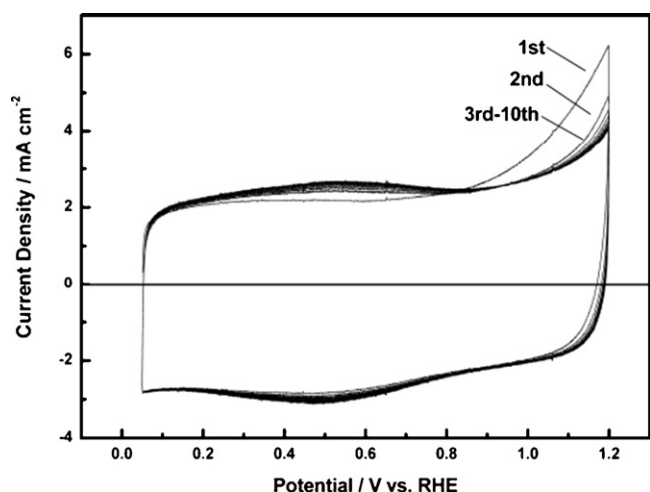
Fig. 3. Cyclic voltammograms (CVs) of the ZrO_xN_y/C catalyst in 0.5 M H_2SO_4 under N_2 atmosphere at room temperature. Sweep rate: 100 mV s^{-1}.

Apparent oxygen reduction currents were observed below ca. 0.9 and 0.75 V versus RHE for sputtered ZrO_2 and ZrO_xN_y, respectively. The onset potential for the ORR on ZrO_xN_y/C electrocatalyst prepared in our study was about 0.7 V versus

RHE, which was comparable to the sputtered ZrO_2 and ZrO_xN_y samples.

The Pt counter electrode is widely used in the conventional three-electrode system to test the electrocatalytic activities of non-precious catalysts as described in the Refs. [20,21]. The potential range of the CV test performed in this work is from 0.05 to 1.2 V versus RHE in the CV test. The Pt counter electrode is very stable in this potential range. As reported by the DOE report 2005 [22], the dissolved platinum equilibrium concentrations form a polycrystalline platinum wire immersed in room-temperature non-adsorbing electrolyte under the voltammetric cycling is below 1.E-07 when the high potential adopted in the cyclic voltammogram is 1.2 V versus RHE. So the dissolved Pt during the CV test will hardly contaminate the working electrode and nearly cannot make the CV results incorrect. Also, the electrolyte is replaced every time when a new catalyst is tested. This will further decrease the influence of the dissolved Pt on the working electrode.

In order to verify whether Pt from the counter electrode will contaminate the working electrode and invalidate the results, we carried out the CV and RDE measurements on ZrO_xN_y/C electrocatalyst in the three-electrode system by the use of graphite rod as the counter electrode. Fig. 5a and b shows the cyclic
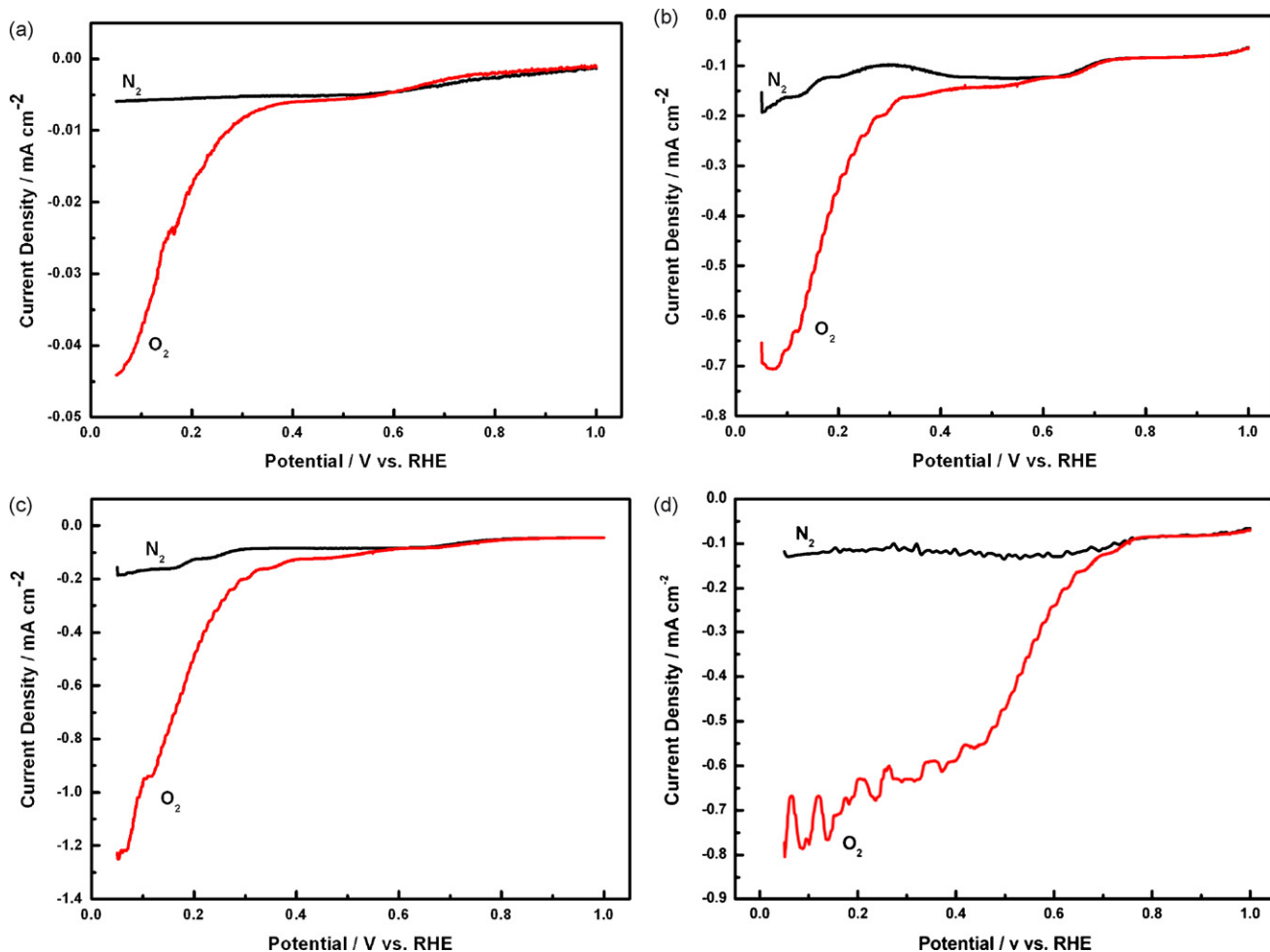

Fig. 4. Linear scan voltammograms (LSVs) of (a) bare GC, (b) XC-72 carbon, (c) ZrO_2/C and (d) ZrO_xN_y/C under N_2 and O_2 atmosphere in 0.5 M H_2SO_4 at room temperature. Sweep direction: negative-going. Sweep rate: 5 mV s^{-1}. Electrode rotation rate: 0 rpm.
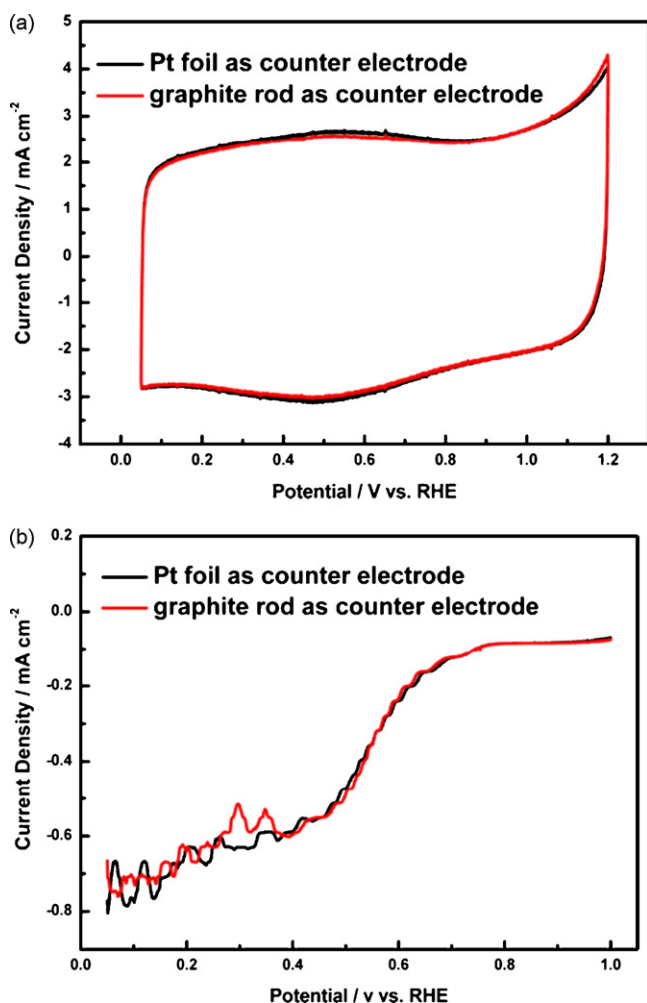
Fig. 5. Comparison of the cyclic voltammograms (a) linear scan voltammograms (b) of ZrO_xN_y/C on RDEs in O_2-saturated 0.5 M H_2SO_4 at room temperature by using Pt foil and graphite rod as the counter electrodes. Sweep rate for CV test: 100 mV s^{-1}; Sweep direction for LSV: negative-going. Sweep rate for LSV: 5 mV s^{-1}. Rotation rate for LSV: 0 rpm.

Fig. 6. Comparison of the linear scan voltammograms for ORR on (a) bare GC, (b) XC-72 carbon (119.05 μg C), (c) ZrO_2/C (23.81 μg ZrO_2), ZrO_xN_y/C (23.81 μg ZrO_xN_y) and Pt/C (23.81 μg Pt) on RDEs in O_2-saturated 0.5 M H_2SO_4 at room temperature. Sweep direction: negative-going. Sweep rate: 5 mV s^{-1}, Electrode rotation rate: 2500 rpm.

voltammograms and linear scan voltammograms on ZrO_xN_y/C electrocatalyst that were processed by using Pt foil and graphite rod as the counter electrodes. The CV and LSV for ORR on ZrO_xN_y/C electrocatalyst that were processed by using graphite rod as the counter electrodes is nearly the same as the test that using Pt foil as the counter electrode. These results truly revealed that Pt from the counter electrode hardly contaminated the working electrode and invalidated the results.

In order to compare the ORR activity more distinctly, the LSV curves of the bare GCE, XC-72 carbon, ZrO_2/C and ZrO_xN_y/C at a constant rotation speed of 2500 rpm in O_2-saturated 0.5 M H_2SO_4 at room temperature were presented in Fig. 6 alongside the LSV curve of 20 wt.% Pt/C (Johnson Matthey). We used negative-going sweeps in our experiment as adopted in Ref. [23]. As described in Ref. [24], Pt surface oxidation will be presented in the negative-going sweeps, which will cause a low activity. But in our work, as elucidated in Fig. 3 (CVs), no specific oxidation and reduction current peaks about the zirconium oxynitride were observed. The negative-going sweeps is
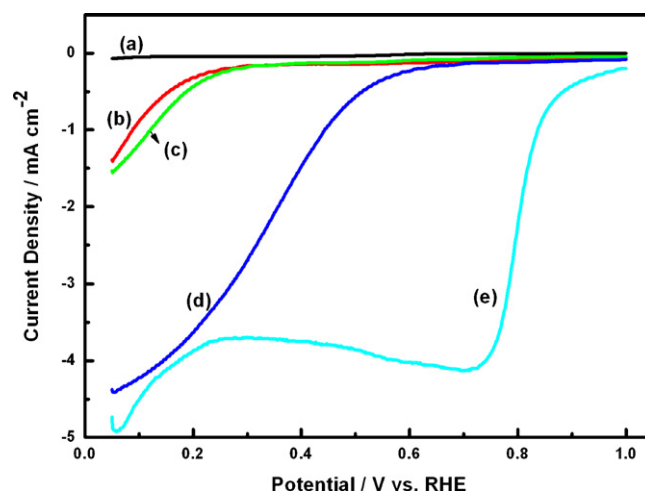
very commonly applied in the detection of polarization curve for a reduction reaction. Meanwhile, all the LSV curves presented in this work were all measured using the negative-going sweeps. So the comparison of the ORR activities among the tested catalysts is unified and the results are credible. As shown in Fig. 6, the bare GCE showed nearly no ORR activity and the ORR activity of ZrO_xN_y/C was far higher than that of XC-72 carbon and ZrO_2/C. Though ZrO_xN_y/C had a clear ORR activity, the onset electrode potential for oxygen reduction catalyzed by ZrO_xN_y/C was much more negative than that catalyzed by Pt/C electrocatalyst. To assure the readers that the experimental setup is functioning properly, the benchmark activity of Pt/C was compared with the Pt activity reported in Refs. [18,24]. The ORR activity of Pt/C reported in this paper is similar to that reported in Ref. [24] and is higher than that reported in Ref. [18]. The tested commercial Pt/C catalyst in this work and the Pt/C catalyst used in Ref. [24] are all carbon-supported Pt catalysts. They both have the similar mean particle size and size distribution. But the Pt catalyst used in Ref. [18] is sputtered Pt and the mean particle size is 30 nm. On the basis of the above comparison of the activities of Pt catalyst, we believe we gave an exact benchmark for the comparison of the ORR activity between the Pt/C catalyst and the synthesized non-noble ZrO_xN_y/C catalyst. The ORR activity of ZrO_xN_y/C could be further improved by optimization of the electrocatalyst composition and the electrochemical active surface.

As seen from Fig. 6, the ORR curve of the thin film ZrO_xN_y/C electrode has no obvious limited current. But we can derive the limited current from Fig. 6. Firstly, the kinetic current at any given potential can be obtained by Koutecky–Levitch (j^{-1} versus $\omega^{-1/2}$) plots, then, according to the following equation:

$$MA = i_{kin} = \frac{i_{lim}i_{obv}}{i_{lim} - i_{obv}} \qquad (2)$$

where i_{lim} is the limited current density, i_{kin} is the kinetic current density, and i is the current density derived from LSV curve.
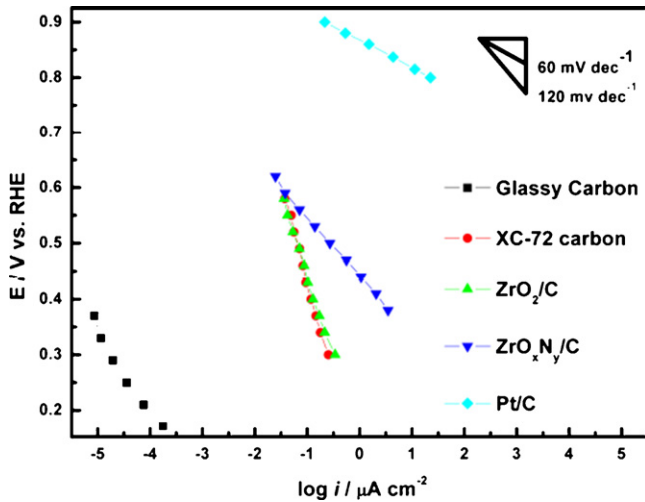
Fig. 7. Tafel plots of the ORR on XC-72 carbon, ZrO$_2$/C, ZrO$_x$N$_y$/C, Pt/C and GC electrodes under O$_2$ atmosphere in 0.5 M H$_2$SO$_4$. Sweep rate: 5 mV s^{-1}. Electrode rotation rate: 2500 rpm. Room temperature.

Fig. 8. Koutecky–Levitch (j^{-1} versus $\omega^{-1/2}$) plots for oxygen reduction on ZrO$_x$N$_y$/C electrocatalyst at different electrode potentials obtained from data of the inset of Fig. 8.

$i_{\lim}$ can be calculated accordingly. From above procedure, the calculated limited current density of the ZrO$_x$N$_y$/C electrode (rotation speed: 2500 rpm) is about 7 mA cm^{-2}, which is higher than that presented in the Ref. [24] (5.5 mA cm^{-2}) at the same rotation speed. But as to ZrO$_x$N$_y$/C electrode, it is difficult for us to measure the limited current directly. We can only make comparisons by the calculated limited current.

Fig. 7 shows the Tafel plots of the ORR on XC-72 carbon, ZrO$_2$/C, ZrO$_x$N$_y$/C, Pt/C and GC electrodes. As seen from Fig. 7, the GC electrode showed nearly no electrocatalytic activity for the ORR. The Tafel slopes of the ORR on XC-72 carbon and ZrO$_2$/C are 293 and 233 mV dec^{-1}, respectively. The above two samples showed poor electrocatalytic activity for the ORR. ZrO$_x$N$_y$/C was found to have a clear electrocatalytic activity for the ORR as we mentioned above. The Tafel slope of the ORR on ZrO$_x$N$_y$/C is 109 mV dec^{-1}. However, the Tafel slope of the ORR on Pt/C is 56 mV dec^{-1}. In comparison with Pt/C, the ORR activity of ZrO$_x$N$_y$/C should be further improved.

To testify the oxygen reduction mechanism of ZrO$_x$N$_y$/C, the Koutecky–Levich equation [21] was used to determine the number of electrons transferred per O$_2$ molecule.

$$-\frac{1}{I} = -\frac{1}{I_K} + \frac{1}{0.62 n F A D^{2/3} c v^{-1/6} \omega^{1/2}} \tag{3}$$

where I_K, the kinetic current; ω, the rotation rate; n, the number of electrons involved in the reaction; F, Faraday constant; A, the geometric area of the disk electrode; D and c are the diffusion coefficient of dissolved oxygen and the concentration of dissolved oxygen in 0.5 M H$_2$SO$_4$, respectively; v is the kinematic viscosity of the electrolyte. Fig. 8 shows Koutecky–Levitch (j^{-1} versus $\omega^{-1/2}$) plots for O$_2$ reduction on ZrO$_x$N$_y$/C electrodes at different electrode potentials in 0.5 M H$_2$SO$_4$. The inset in Fig. 8 shows the LSV curves of the ZrO$_x$N$_y$/C electrocatalyst obtained at various rotations rates on a GCE. The number of electrons transferred per O$_2$ molecule was determined by Eq. (2) according to the data of the inset figure in Fig. 8. The linearity of the plots confirmed the applicability of Eq. (2) to
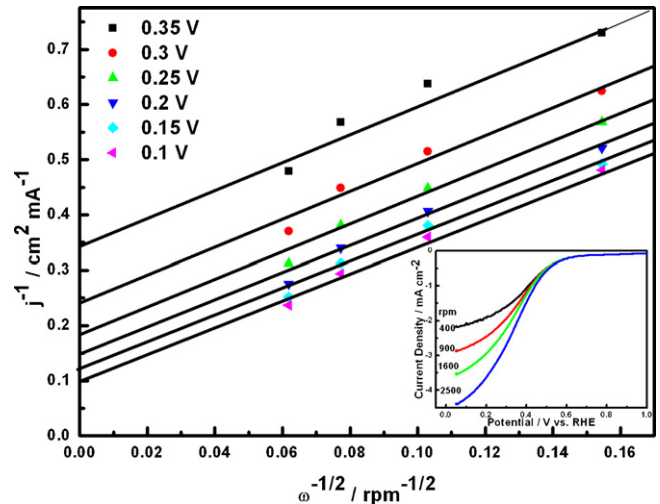
analysis of the behavior at the electrocatalyst layer. The calculation of n was performed using the values: F, 96485 C mol^{-1}; A, 0.1256 cm^2; D, 1.93 × 10^{-5} cm^2 s^{-1}; c, 1.13 × 10^{-6} mol cm^{-3}; v, 9.5 × 10^{-3} cm^2 s^{-1} [25]. The number of electrons is 3.8, close to 4. This suggested that the molecular oxygen was directly reduced to water on the surface of ZrO$_x$N$_y$/C. Further investigation using a rotating ring-disk electrode will be reported in the future work to confirm the four-electron pathway.

There has been considerable interest in the electrocatalytic properties of transition-metal nitrides and they were found to have high activities similar to those of noble metal electrocatalysts in isomerization, hydrogenation, dehydrogenation and water gas shift reactions [26,27]. The noble metal-like properties of the ZrO$_x$N$_y$/C electrocatalyst is of major importance for the attractive ORR activity. Meanwhile, zirconium oxide has been found to have some ORR activity [18]. The crystallinity of ZrO$_x$N$_y$/C was better than ZrO$_2$/C, this would be one of the factors to affect the catalytic activity for ORR [19].

3.3. Single cell tests

The single cell performances achieved at 40, 60 and 80 °C with ZrO$_x$N$_y$/C as cathode electrocatalyst were shown in Fig. 9. The cell performances of ZrO$_2$/C and Pt/C as cathode electrocatalyst at 80 °C were also shown in Fig. 9 for giving a good comparison. The ZrO$_2$/C sample showed the worst cell performance among the three tested catalysts with the maximum power density of 10.7 mW cm^{-2}. The maximum power density (50 mW cm^{-2}) of the single cell based on ZrO$_x$N$_y$/C as cathode electrocatalyst achieved at 80 °C was far lower than the single cell based on commercial Pt/C as cathode electrocatalyst (570 mW cm^{-2}). In addition, as described by Jaouen et al. in ref. [28], the state-of-the-art non-Pt ORR catalyst (nitrogen-doped carbon-supported Fe) also showed a better cell performance than ZrO$_x$N$_y$/C catalyst in this work. The ORR activity of the ZrO$_x$N$_y$/C catalyst should be further improved. However, as shown in Fig. 9, the MEA operated at 80 °C gave a better per-
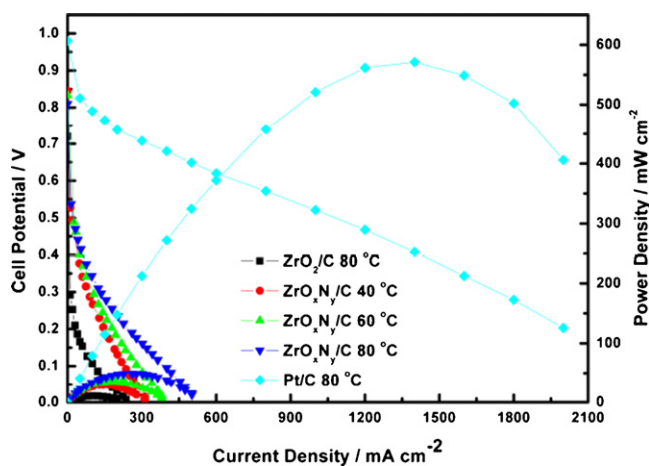
Fig. 9. Performance curves of single cell adopting ZrO_2/C, ZrO_xN_y/C and Pt/C as cathode electrocatalyst at different temperatures. Anode: the commercial TKK 46.6% Pt/C electrocatalyst with Pt loading of $0.37\,mg\,cm^{-2}$. Cathode: ZrO_2 and ZrO_xN_y loading are all $1\,mg\,cm^{-2}$; Pt loading is $0.4\,mg\,cm^{-2}$. $H_2/O_2 = 0.2\,MPa/0.2\,MPa$. Pure hydrogen and oxygen are put into the cell with saturated humidification. Flow rates of H_2 and O_2 are $50\,ml\,min^{-1}$ and $100\,ml\,min^{-1}$, respectively.

formance than that operated at 60 and 40 °C. At the current density of $200\,mA\,cm^{-2}$, the cell voltage is 0.238 V, which is about 63 and 106 mV higher than that at 60 and 40 °C, respectively. These initial results indicated that the MEA performance could be improved when operated at a higher temperature. And also, better performance can be obtained by optimization in the electrocatalyst preparation process and the MEA manufacture.

3.4. Stability test

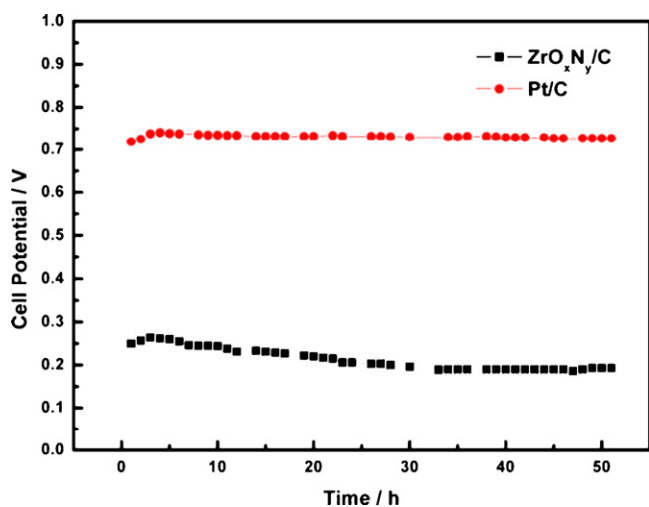The stability test of the ZrO_xN_y/C and Pt/C electrocatalysts had been conducted on single cells operated at 80 °C.

Fig. 10. Stabilities of ZrO_xN_y/C and Pt/C as cathode electrocatalysts in single cells at the constant current density of $200\,mA\,cm^{-2}$. Anode: the commercial TKK 46.6% Pt/C electrocatalyst with Pt loading of $0.37\,mg\,cm^{-2}$. Cathode: ZrO_xN_y loading is $1\,mg\,cm^{-2}$; Pt loading is $0.4\,mg\,cm^{-2}$. Cell temperature: 80 °C. $H_2/O_2 = 0.2\,MPa/0.2\,MPa$. Pure hydrogen and oxygen are put into the cell with saturated humidification. Flow rates of H_2 and O_2 are $50\,ml\,min^{-1}$ and $100\,ml\,min^{-1}$, respectively.

Fig. 10 shows the stabilities of the single cells using ZrO_xN_y/C and Pt/C as the cathode electrocatalysts at a constant current density of $200\,mA\,cm^{-2}$. For the Pt/C electrocatalyst, the cell voltage changed a little during the whole operating time. For the ZrO_xN_y/C electrocatalyst, the cell voltage decreased about 25 mV in the initial 20 h. Then, the cell voltage maintained almost the same value during the following test time. It should be noted that the parameters for the cathode electrocatalyst layer formation were not optimized. The parameters are, for instance, the loading of the ZrO_xN_y/C electrocatalyst and the proton conducting electrolyte, the microstructures of the diffusion layer and the electrocatalyst layer. These parameters would influence the stability of the cell performance [29]. In addition, the optimization of nitrogen content in zirconium oxynitride and zirconium oxynitride loading on the carbon support would also improve the activity and durability. Further studies are required and are currently underway.

4. Conclusion

In this work, carbon-supported zirconium oxynitride as a noble-metal-free ORR electrocatalyst was prepared by ammonolysis of ZrO_2/C at 950 °C. This non-noble electrocatalyst showed a good stability in acid media and presented a promising electrocatalytic activity for the ORR with an approximate four-electron process. The performance achieved by the H_2/O_2 single cell is most related to the intrinsic properties of the ZrO_xN_y/C electrocatalyst, and could be improved by the optimization of the electrocatalyst preparation process, the MEA manufacture and the operating conditions. Further optimization for the electrocatalyst preparation and the long-term single cell test are under way. The zirconium oxynitride might possibly be a substitute material for the platinum cathode of PEMFCs.

Acknowledgement

References

[1] A.K. Shukla, P.A. Christensen, A. Hamnett, M.P. Hogarth, J. Power Sources 55 (1995) 87.
[2] L. Xiong, A. Manthiram, Electrochim. Acta 50 (2005) 2323.
[3] H. Yang, W. Vogel, C. Lamy, N. Alonso-Vante, J. Phys. Chem. B 108 (2004) 11024.
[4] S. Litster, G. Mclean, J. Power Sources 130 (2004) 61.
[5] U.A. Paulus, A. Wokaun, G.G. Scherer, J. Phys. Chem. B 106 (2002) 4181.
[6] H.R. Colón-Mercado, H. Kim, B.N. Popov, Electrochem. Commun. 6 (2004) 795.
[7] H.R. Colón-Mercado, B.N. Popov, J. Power Sources 155 (2006) 253.
[8] B. Wang, J. Power Sources 152 (2005) 15.
[9] H.A. Gasteiger, S.S. Kocha, B. Sompalli, F.T. Wagner, Appl. Catal. B: Environ. 56 (2005) 9.
[10] L. Zhang, J.J. Zhang, D.P. Wilkinson, H.J. Wang, J. Power Sources 156 (2006) 171.
[11] P.K. Ajikumar, M. Kamruddin, R. Nithya, P. Shankar, S. Dash, A.K. Tyagi, B. Raj, Scripta Mater. 51 (2004) 361.
[12] W.J. Chou, G.P. Yu, J.H. Huang, Surf. Coat. Technol. 167 (2003) 59.

[13] F. Mazza, S. Trassatti, J. Electrochem. Soc. 110 (1963) 847.

[14] H.X. Zhong, H.M. Zhang, G. Liu, Y.M. Liang, J.W. Hu, B.L. Yi, Electrochem. Commun. 8 (2006) 707.

[15] J.C. Gilles, R. Collongues, C. R. Acad. Sci. 254 (1962) 1084.

[16] M. Bhagwat, V. Ramaswamy, Mater. Res. Bull. 39 (2004) 1627.

[17] M. Lerch, J. Mater. Sci. Lett. 17 (1998) 441.

[18] Y. Liu, A. Ishihara, S. Mitsushima, N. Kamiya, K. Ota, Electrochem. Solid State Lett. 8 (8) (2005) A400.

[19] S. Doi, Y. Liu, A. Ishihara, S. Mitsushima, N. Kamiya, K. Ota, J. Electrochem. Soc. 154 (3) (2007) B362.

[20] F. Jaouen, M. Lefèvre, J.P. Dodelet, M. Cai, J. Phys. Chem. B 110 (2006) 5553.

[21] S. Ye, A.K. Vijh, J. Solid State Electrochem. 9 (2005) 146.

[22] D. Myers, X.P. Wang, R. Kumar, DOE Hydrogen Program FY 2005 Progress Report, Cathode Electrocatlysis: Platinum Stability and Non-Platinum Electrocatalysts.

[23] N.P. Subramanian, S.P. Kumaraguru, H. Colon-Mercado, H. Kim, B.N. Popov, T. Black, D.A. Chen, J. Power Sources 157 (2006) 56.

[24] U.A. Paulus, T.J. Schmidt, H.A. Gasteiger, R.J. Behm, J. Electroanal. Chem. 495 (2001) 134.

[25] M.S. El-Deab, T. Ohsaka, Electrochim. Acta 47 (2002) 4255.

[26] U.S. Ozkan, L. Zhang, P.A. Clark, J. Catal. 172 (1997) 294.

[27] S. Li, W.B. Kim, J.S. Lee, Chem. Mater. 10 (1998) 1853.

[28] F. Jaouen, F. Charreteur, J.P. Dodelet, J. Electrochem. Soc. 153 (4) (2006) A689.

[29] J. Maruyama, I. Abe, Chem. Mater. 17 (2005) 4660.